Intersubunit Association Induces Unique Allosteric Dependence of the T127L CRP Mutant on pH†

Ying Shi, Shenglun Wang, and Frederick P. Schwarz*

Center for Advanced Research in Biotechnology/National Institute of Standards and Technology, 9600 Gudelsky Drive, Rockville, Maryland 20850

Received February 2, 2000; Revised Manuscript Received April 19, 2000

ABSTRACT: The allosteric activation of the T127→L mutant of 3′,5′-cyclic adenosine monophosphate (cAMP) receptor protein (CRP) by cAMP changes from an exothermic, independent two-site binding mechanism at pH 7.0 to an endothermic, interacting two-site binding mechanism at pH 5.2, similar to that observed for CRP at pH 7.0 and 5.2. Since the T127→L mutation at the subunit interface of the CRP dimer creates a more perfect leucine-zipper motif, it is believed to increase the intersubunit association and the stability of the CRP, as is observed by the higher thermal stability of the T127L mutant relative to that of CRP in differential scanning calorimetry (DSC) measurements. The DSC scans also exhibit a single thermal denaturation transition for CRP and a S128A mutant from pH 5.2 to 7.0, while the broader transition peak of the T127L mutant becomes resolvable into two transitions below pH ≤5.2. Circular dichroism measurements on T127L and CRP at pH 7.0 and 5.2 show changes in the tertiary structure of both proteins with the exception of the tertiary structure around the two tryptophan residues in the amino-terminal domain. Although gel electrophoresis of the proteolysis (pH 5.2) products of T127L, CRP, and their cAMP- and cGMP-ligated complexes shows the subunit band and an amino-terminal domain fragment band, the fully allosterically activated complexes of T127L and CRP show the amino-terminal domain fragment band but not the subunit band. The results are interpreted in terms of the allosteric activation of CRP by cAMP by a conformational change from an "open" to a "closed" form of CRP, which involves changes in the tertiary structure of the carboxyl-terminal domains that are partially induced by an increase in the intersubunit association in T127L. While T127L retains its intersubunit association from pH 5.2 to 7.0, changes occur in the carboxyl-terminal domain so that the endothermic, allosteric activation mechanism of CRP by cAMP is restored in T127L at pH 5.2.

Allosteric activation of 3′,5′-cyclic adenosine monophosphate (cAMP)[1] receptor protein (CRP) by cAMP results in the enhancement of the transcription of over 25 operons, which code for enzymes involved in catabolite metabolism. CRP consists of two 22 500 g mol^{-1} identical subunits, with an α-helical motif along the monomer−monomer interface between the amino- and carboxyl-terminal domains of each subunit (*1*). Allosteric activation of CRP is initiated by the binding of cAMP to the amino-terminal domains of CRP, which then activates a conformational change in CRP so that its carboxyl-terminal domains bind to a site in the promoter region of the operon, adjacent to the RNA polymerase binding site. Single amino acid substitutions at the α-helical monomer−monomer interface of CRP significantly alter the allosteric activation of CRP by cAMP (*2*, *3*). A S128→A mutation, which eliminates a crossover interaction between the 128 residue in one subunit and cAMP in the other subunit (*1*), reduces the allosteric activation of CRP by cAMP (*2*, *3*). Mutations of T127 to L (*2*), C, I, and S (*3*) resulted in the allosteric activation of CRP by 3′,5′-cyclic guanosine monophosphate (cGMP), an analogue of cAMP. The level of allosteric activation by the T127I and T127S mutants of CRP, however, was found to be much lower than that of CRP and T127C in the presence of cAMP (*4*). It was concluded that the changes in the allosteric activation of the T127 mutants resulted from differences in the reorientation of the DNA binding helices in the carboxyl-terminal domain induced by these mutations (*4*). Both the T127→ L mutation, which converts the α-helical interface to a more perfect leucine-zipper motif, and the T127→C mutation, which forms a disulfide bond across the subunit interface, very possibly strengthen the intersubunit association, and this could contribute to the conformational change that is responsible for the allosteric activation of CRP by cAMP. This would be consistent with the observation that the binding of cAMP to CRP reduces the intersubunit dissociation of CRP at low concentrations (*5*). In addition, T127L binds to a promoter consensus site sequence (*6*) and activates in vitro transcription in the absence of a cyclic nucleoside monophosphate (cNMP), while CRP and the S128A mutant still require

† This work was supported by National Science Foundation Grant MCB-9722884 to F. P. S.

* To whom correspondence should be addressed. Telephone: 301-738-6219, FAX: 301-738-6255, email: fred@carb.nist.gov.

[1] Abbreviations: cAMP, 3′,5′-cyclic adenosine monophosphate; CD, circular dichroism; cGMP, 3′,5′-cyclic guanosine monophosphate; cNMP, cyclic monophosphate nucleoside; CRP, cAMP receptor protein; DSC, differential scanning calorimeter; DTT, dithiothreitol; EDTA, sodium ethylenediaminetetraacetate; ITC, isothermal titration calorimetry; SANS, small-angle neutron scattering; S128A, S128→A mutant of CRP; T127L, T127→L mutant of CRP.

10.1021/bi000225m
Published on Web 05/25/2000

cAMP for allosteric activation (unpublished results). Although subunit realignment by mutations near the interface has been considered important in the allosteric activation of CRP (*7*), the specific role of stronger intersubunit association in the structural changes resulting in the allosteric activation of CRP needs to be elucidated.

In this study, the unique allosteric activation of T127L by cAMP and cGMP was investigated in more detail by isothermal titration calorimetry measurements (ITC) as a function of pH and temperature. Previous ITC studies (*8*) showed that the allosteric activation of CRP by cAMP at pH 7.0 is achieved by a cooperative binding mechanism consisting of exothermic cAMP binding to the first subunit of CRP, which enhances endothermic binding to the second subunit of CRP. At low cAMP concentrations, it was shown that the allosteric activation of CRP could also be achieved by cAMP binding to the first subunit (*6*). The allosteric activation of the T127L and S128A mutants by cAMP and cGMP, however, is exothermic and is achieved by a noncooperative, independent two-site binding mechanism (*8*, *9*). It was concluded that the endothermic binding of cAMP to the second subunit of CRP results from a large conformational change in cAMP-ligated CRP in addition to the more subtle conformational change involved in the allosteric activation of CRP. In the present investigation, it was observed that the cAMP binding mechanism to CRP, consisting of exothermic binding to the first subunit and endothermic binding to the second subunit, is partially restored in T127L at low pH and at 38 °C. Differential scanning calorimetry measurements (DSC), circular dichroism measurements (CD), and proteolysis by subtilisin were employed to determine the effect of pH on the initial and final conformations of T127L and CRP, which would account for the unique allosteric activation of T127L by cAMP. Differences in the conformations are discussed in terms of the effect on the structural changes induced in the allosteric activation of CRP by stronger intersubunit association through the T127→L mutation at the subunit interface.

EXPERIMENTAL PROCEDURES

Materials. The production of CRP and mutants from *E. coli* and their subsequent purification have been described previously (*2*). Their activities were checked by an in vitro transcription assay as described by Zhang et al. (*10*). Following extensive dialysis in the appropriate buffer, the protein concentrations were determined from UV measurements at 280 nm using an extinction coefficient of 3.5×10^4 M^{-1} cm^{-1} (*9*). At pH 7.0, the buffer was 0.05 M K_2HPO_4/KH_2PO_4 + 0.5 M KCl + 0.2 mM EDTA + 0.2 mM DTT + 5 vol % glycerol while at pH ≤5.2 0.05 M $KC_2H_3O_2$/$C_2H_4O_2$ was substituted for the potassium phosphate salts. The potassium phosphate and acetate salts, acetic acid, KCl, and the sodium salts of cAMP, cGMP, and cIMP were reagent grade from Sigma Chemical Co.[2] To match the titrant buffer with that of the protein solution in the ITC measurements, the titrant solutions were made up by dissolving the sodium salt of cNMP in the buffer dialysate from dialysis of the protein solution. The concentrations of the cNMP solutions were determined by using an extinction coefficient of 1.23×10^4 M^{-1} cm^{-1} at 260 nm for cAMP and 1.34×10^4 M^{-1} cm^{-1} at 250 nm for cGMP (*8*). The 40 base pair consensus DNA duplex was made up by annealing the two single strand complementary DNA sequences obtained from Oligos, Inc., according to the procedure described previously (*6*). The consensus DNA duplex ligand solution was dialyzed in the same buffer as the protein solution and its concentration determined by using an extinction coefficient at 260 nm of 1.32×10^4 M^{-1} cm^{-1} per base pair. The DTT was ultrapure brand from GIBCOBRL, and the EDTA was from Serva Co.

Isothermal Titration Calorimetry. All calorimetric titrations were performed according to the methods of Wiseman et al. (*11*) and Gorshkova et al. (*8*) using a Microcal Omega titration calorimeter. The Omega titration calorimeter consists of a matched pair of sample and reference vessels (1.374 mL) containing the protein in buffer solution and the buffer solution, respectively. Aliquots (4−10 μL) of the ligand solution at concentrations 10−20× the protein concentration of 0.1−0.5 mM in the sample vessel were added 3−4 min apart. A separate titration of the ligand solution into the buffer was performed to determine any ligand heat of dilution, which was then subtracted from the heats obtained during the titration of the ligand solution into the protein solution.

A nonlinear, least-squares minimization performed by Microcal ORIGIN scientific plotting software was used to fit the incremental heat of the ith titration [$\Delta Q(i)$] of the total heat, Q_t (*12*):

$$\Delta Q(i) = Q(i) + \mathrm{d}Vi/2V\{[Q(i) + Q(i-1)] - Q(i-1)\} \quad (1)$$

For an identical independent two-site binding mechanism:

$$Q_t = n[C_t]\Delta H_b^\circ V\{1 + [X_t]/n[C_t] + 1/nK_b[C_t] - [(1 + [X_t])/n[C_t] + 1/nK_b[C_t]^2 - 4[X_t]/n[C_t]]^{1/2}\}/2 \quad (2)$$

where $n = 2$, the stoichiometry of the binding reaction, $[C_t]$ is the total CRP concentration in the sample vessel, ΔH_b is the binding enthalpy, $[X_t]$ is the total cNMP ligand concentration, and K_b is the binding constant. For the interacting two-site mechanism:

$$Q_t = C_t V\{K_b(1)[X_t]\Delta H_b^\circ(1) + K_b(1)K_b(2)[X_t]^2[\Delta H_b^\circ(1) + \Delta H_b^\circ(2)]\}/P \quad (3a)$$

where

$$P = 1 + K_b(1)[X_t] + K_b(1)K_b(2)[X_t]^2 \quad (3b)$$

$K_b(1)$ and $\Delta H_b^\circ(1)$ are the binding constant and enthalpy for binding to the first site, and $K_b(2)$ and $\Delta H_b^\circ(2)$ are the binding constant and enthalpy for binding to the second site. The ORIGIN program yields the on-site binding constants, and, thus, the binding constants reported in this paper are the on-site binding constants. The macroscopic binding constants to the first site and to the second site are, respectively, $2K_b(1)$ and $K_b(2)/2$, where for the identical site mechanism, $K_b(1) = K_b(2)$. The coefficient of cooperativity,

[2] Certain commercial equipment, instruments, and materials are identified in this paper in order to specify the experimental procedure as completely as possible. In no case does this identification imply a recommendation or endorsement by the National Institute of Standards and Technology, nor does it imply that the material, instrument, or equipment identified is necessarily the best available for the purpose.

Table 1: Thermodynamic Quantities of cAMP and cGMP Binding to CRP, T127L, and S128A at pH 7.0 and 5.2[a,b]

CRP	cNMP	pH	T (°C)	K_b[c] ($\times 10^4$ M^{-1})	$-\Delta G_b°$ (kJ mol^{-1})	$\Delta H_b°$ (kJ mol^{-1})	$\Delta S_b°$ (J mol^{-1} K^{-1})
CRP	cAMP	5.2	24.5	2.0 ± 0.3	24.4 ± 0.3	−5.9 ± 0.5	62 ± 2
				0.82 ± 0.07	22.3 ± 0.2	30.4 ± 0.9	177 ± 3
CRP	cAMP	5.2	36.4	2.2 ± 0.4	25.8 ± 0.5	−8.1 ± 1.2	57 ± 4
				2.6 ± 0.2	26.2 ± 0.2	44.2 ± 1.2	221 ± 4
CRP	cAMP	7.0	24.0	2.9 ± 0.4	25.5 ± 0.3	−5.6 ± 0.6	67 ± 18
				14.0 ± 1.0	29.3 ± 0.2	48.1 ± 2.1	261 ± 10
CRP	cAMP	7.0	39.3	5.1 ± 1.5	31.7 ± 0.9	−10.1 ± 2.6	69 ± 8
				26 ± 8	32.4 ± 0.9	25.4 ± 2.5	185 ± 8
T127L	cAMP	5.2	23.8	0.13 ± 0.03	17.7 ± 0.5	11.6 ± 1.5	98 ± 5
				0.016 ± 0.003	12.4 ± 0.4	26.2 ± 1.5	129 ± 5
T127L	cAMP	5.2	38.2	0.44 ± 0.05	21.7 ± 0.2	−2.1 ± 0.2	62 ± 1
				0.55 ± 0.03	22.3 ± 0.1	32.3 ± 0.4	174 ± 1
T127L	cAMP	7.0	24.0	8.0 ± 3.0	27.9 ± 0.9	−3.4 ± 0.1	82 ± 3
T127L	cAMP	7.0	39.5	3.3 ± 1.0	27.1 ± 0.8	−10.5 ± 2.1	53 ± 7
T127L	cGMP	5.2	23.0	0.99 ± 0.12	22.6 ± 0.2	−7.3 ± 1.1	51 ± 5
T127L	cGMP	5.2	37.3	1.4 ± 0.3	24.6 ± 0.4	−20.8 ± 3.2	13 ± 10
T127L	cGMP	7.0	24.0	2.8 ± 0.9	25.3 ± 1.1	−5.8 ± 1.4	66 ± 6
T127L	cGMP	7.0	39.5	2.5 ± 0.3	26.3 ± 0.3	−17.2 ± 1.3	34 ± 4
S128A	cAMP	5.2	23.7	5.0 ± 0.3	26.7 ± 0.3	−14.9 ± 0.5	39 ± 2
S128A	cAMP	5.2	37.3	14.2 ± 0.5	24.6 ± 0.1	−26.8 ± 1.3	−7 ± 5
S128A	cAMP	7.0	24.0	12.4 ± 0.1	29.0 ± 0.1	−10.4 ± 1.2	62 ± 4
S128A	cAMP	7.0	39.0	7.8 ± 0.3	29.2 ± 0.1	−23.4 ± 0.9	19 ± 3

[a] The uncertainties are standard uncertainties as defined in the text. [b] The values at pH 7.0 are from references *8* and *9*. [c] For the interacting two-site binding mechanism, the first set of quantities are for on-site binding to the first subunit and the second set are for on-site binding to the second subunit. For the independent two-site binding mechanism, only one set of on-site binding thermodynamic quantities are given since they are identical for the two subunits.

α, for the two-site model is defined as the ratio of $K_b(2)/K_b(1)$ and the energy of interaction as $\Delta G = -RT \ln \{\alpha\}$. The binding entropies, $\Delta S_b°$, were calculated using the following equation of thermodynamics:

$$\Delta S_b° = (\Delta H_b° - \Delta G_b°)/T \quad (4)$$

The combined standard uncertainties in K_b and $\Delta H_b°$ were estimated to be each 1.1% from the standard uncertainties in $[C_t]$, $[X_t]$, Q, and V. This accounts for the standard deviation in the mean value of $\Delta H_b°$ from several titration scans. However, this combined estimated uncertainty is less than the standard deviation in the mean values of K_b from several titration runs as shown in Table 1.

Differential Scanning Calorimetry. DSC measurements were performed from 8 to 20 K h^{-1} with a Hart 7707 DSC heat conduction scanning microcalorimeter as described by Schwarz and Kirchhoff (*13*). The Hart DSC consists of four removable vessels contained in an adiabatic enclosure with three of the vessels containing samples of the protein solution and the fourth vessel containing just the buffer solution. The sample size was 0.500 g, and most of the samples were scanned at 13 K h^{-1} from 30 to 90 °C. DSC measurements were also performed at a scan rate of 80 K h^{-1} with a Microcal, Inc., VP DSC, which consists of a matched pair of fixed 0.511 mL solution vessel and reference vessel enclosed in an adiabatic enclosure. The operating procedure of the VP DSC is described by Chakrabarti and Schwarz (*14*). Thermal power versus temperature scans of buffer versus buffer were subtracted from the solution versus buffer power scans to obtain the net power scans which were then divided by the scan rate to convert the net power scans to excess heat capacity vs temperature scans using EXAM (*15*). EXAM was used to extrapolate a sigmoidal baseline under the transition peak and to fit a two-state transition model to the data points to obtain the transition temperature (T_m, the temperature at half the peak area), a van't Hoff enthalpy ($\Delta_{trs}H_v$) for the transition, and the area under the transition peak. The transition peak area divided by the number of moles of protein in the sample yielded the calorimetric enthalpy, $\Delta_{trs}H_c$. With two overlapping transition peaks, a straight-line baseline was extrapolated under the transition peaks, the data pertaining to the second transition peak were erased, and the two-state transition model was fitted to the data for the first transition peak. The data pertaining to the second transition peak were then restored, and the transition model-fitted peak was subtracted from the data to obtain data pertaining only to the second transition peak. The two-state transition model was then fitted to the data for the second peak, and this procedure was continued until the superposition of the two model peaks fitted very closely all the data points and further continuation of this procedure did not improve the fit of the models to the data.

The standard uncertainty in T_m determined from imprecision in the temperature readings and imprecision in the fractional areas under the transition peak is estimated to be ±0.1 K. The combined estimated uncertainty in the van't Hoff enthalpy from imprecision in the fractional area under the transition peak was estimated to be 3%.

The combined estimated uncertainty in $\Delta_{trs}H_c$ contains uncertainty contributions from the area under the transition peak, the concentration of protein, the sample mass, and the heat calibration of the DSC and is 3.2%. As shown in Table 2, the standard deviations of the mean values of $\Delta_{trs}H_v$ and $\Delta_{trs}H_c$ are greater than the combined estimated uncertainties of these values.

Circular Dichroism Measurements. Circular dichroism (CD) measurements were performed with a Jasco J-720 spectropolarimeter using water-jacketed cells with a path length of 0.1 cm for near-UV measurements (350−250 nm) and of 0.1 mm for far-UV measurements (250−190 nm). Temperature control was provided by a Neslab RTE-110 circulating water bath interfaced with a MTP-6 programmer.

Table 2: Thermodynamic Cooperative Binding Parameters and Heat Capacity Changes for cAMP Binding to CRP and T127 L[a]

protein	pH	T (°C)	α	$\Delta G(\alpha)$ (kJ mol^{-1})	ΔC_{p1} (kJ mol^{-1} K^{-1})	ΔC_{p2} (kJ mol^{-1} K^{-1})
CRP	7.0	24.0	4.8 ± 0.7	-3.9 ± 0.4		
CRP	7.0	39.3	4.0 ± 1.2	-3.6 ± 0.8	-0.30 ± 0.08	-1.47 ± 0.17
CRP	5.2	24.5	0.40 ± 0.07	2.3 ± 0.4		
CRP	5.2	36.4	1.2 ± 0.3	0	-0.18 ± 0.11	1.15 ± 0.13
T127L	7.0	24.0	1.0 ± 0.2	0		
T127L	7.0	39.5	1.0 ± 0.2	0	-0.47 ± 0.15	-0.47 ± 0.15
T127L	5.2	23.8	0.12 ± 0.03	5.2 ± 0.6		
T127L	5.2	38.2	1.3 ± 0.1	-0.8 ± 0.2	-0.95 ± 0.10	0.42 ± 0.10

[a] The values at pH 7.0 are from reference *8*. The uncertainties are standard uncertainties as described in the text.

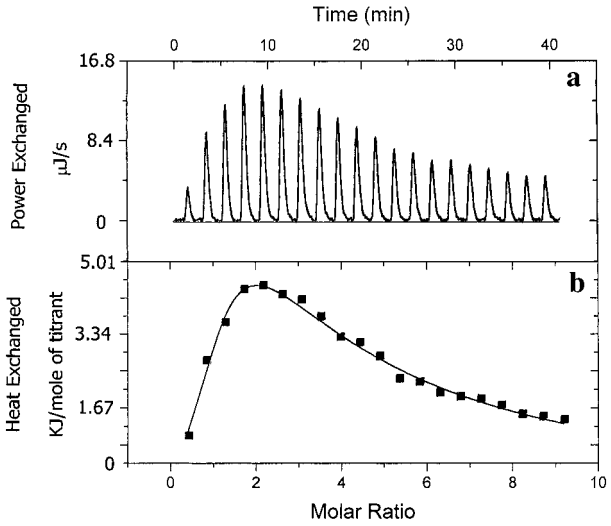

FIGURE 1: (a) ITC titration of 5 μL aliquots of 10 mM cAMP into 0.168 mM T127L in acetate buffer at pH 5.2 and 38 °C. (b) The binding isotherm for the titration in (a) where the solid line is the fit of the data to an interacting two-site binding model.

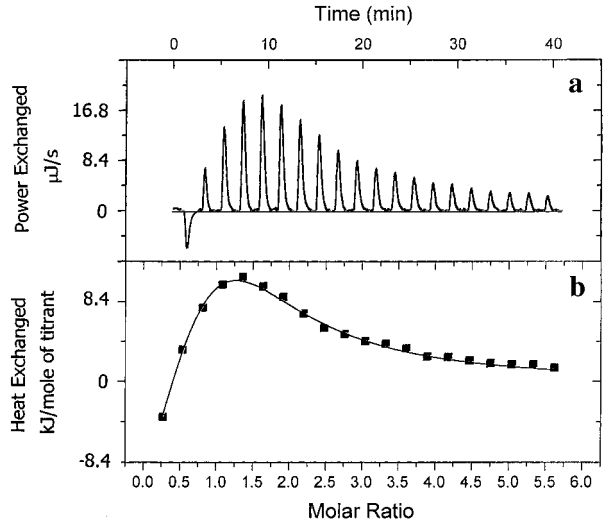

FIGURE 2: (a) ITC titration of 5 μL aliquots of 10 mM cAMP into 0.133 mM CRP in acetate buffer at pH 5.2 and 36.4 °C. (b) The binding isotherm for the titration in (a) where the solid line is the fit of the data to an interacting two-site binding model.

The reported CD spectra represent the averages of five scans, and the results were expressed as mean residue ellipticity, [θ], in deg cm^{-2} dmol^{-1}. The concentration of CRP and T127L was 0.25 mM, and the recording temperature was 24 °C. The uncertainty of the CD data is about 3% and arises principally from uncertainty in the concentrations since the imprecision of the scans is less than 0.1%.

Proteolysis Products. The proteolysis of the T127L and CRP in the absence and presence of cNMP was performed as described prevously (*2*). The proteins were dialyzed against the 0.05 M $KC_2H_3O_2/C_2H_4O_2$ buffer containing 2.5 mM $MgCl_2$, 0.1 mM EDTA, and 100 mM KCl. Twenty-four microliter reaction mixtures containing 10 μg of the CRP/mutant, 1 μg of subtilisin, 0.100 mM cAMP or cGMP were incubated at 37 °C for 20 min. The reactions were terminated by the addition of phenylmethylsulfonyl fluoride. Sodium dodecyl sulfate electrophoresis gels were run on the reaction mixtures.

RESULTS

ITC Measurements. Typical results of titrating 5 μL aliquots of a cAMP solution into a solution of T127L at 38 °C and pH 5.2 are shown in Figure 1 along with the binding isotherm. The allosteric activation of T127L by cAMP in Figure 1 is endothermic and involves an interacting two-site binding mechanism, as is also observed for the cAMP activation of CRP at pH 5.2 in Figure 2 and at pH 7.0 reported previously (*8*). This is in contrast to the allosteric

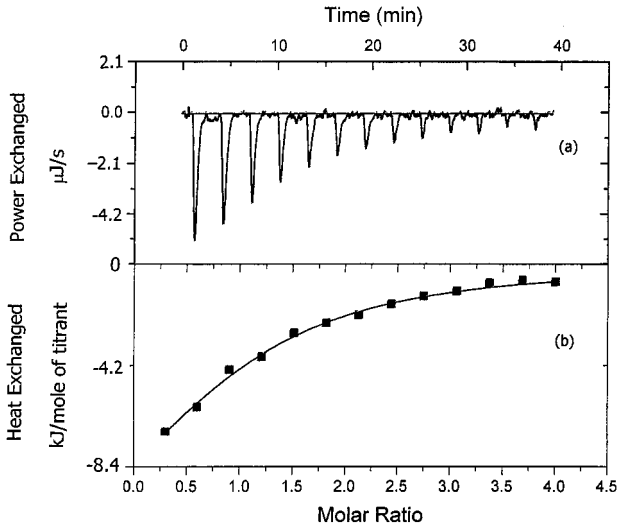

FIGURE 3: (a) ITC titration of 5 μL aliquots of 10 mM cAMP into 0.080 mM T127L in phosphate buffer at pH 7.0 and 38 °C. (b) The binding isotherm for the titration in (a) where the solid line is the fit of the data to a two-site independent binding model.

activation of T127L by cAMP at pH 7.0 (Figure 3) and by cGMP at pH 7.0 and 5.2 (Figure 4), which are exothermic and involve an independent two-site binding mechanism. The results of fits of the two types of binding mechanisms to the titration data are presented in Table 1 along with results for the allosteric activation of S128A by cAMP at pH 7.0 and 5.2, which is also exothermic and follows an independent

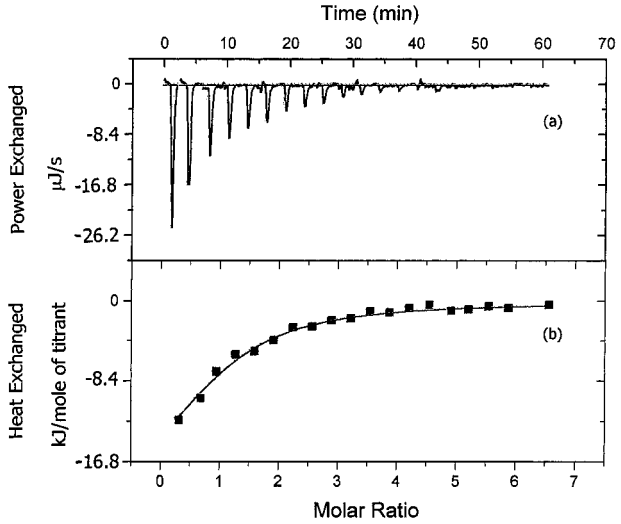

FIGURE 4: (a) ITC titration of 5 μL aliquots of 10 mM cGMP into 0.114 mM T127L in acetate buffer at pH 5.2 and 38 °C. (b) The binding isotherm for the titration in (a) where the solid line is the fit of the data to an independent two-site binding model.

two-site binding mechanism. For the independent two-site binding mechanism of S128A, the site binding constants are reduced by a factor of 2−3 as the pH is reduced from 7.0 to 5.2, resulting mainly from a smaller increase in the binding entropy at the lower pH. For the only endothermic, interacting two-site binding mechanism, which occurs at both pH levels, cAMP binding to CRP, cAMP binding to the first subunit is exothermic with a binding constant which is almost the same at pH 7.0 and pH 5.2, and binding to the second subunit is strongly endothermic with a binding constant which decreases by a factor of 4−9 in going from pH 7.0 to pH 5.2. At the lower temperature, this decrease results from a decrease in the binding entropy, and at the higher temperature, this decrease results from an increase in the endothermic binding enthalpy. These differences in the entropic and enthalpic contributions to $\Delta G_b°$ at the different pH levels and temperatures arise out of significant differences in the heat capacity changes accompanying cAMP binding to the second subunit.

The coefficients of cooperativity, α, and energies of interaction [$-RT \ln(\alpha)$] determined from the results in Table 1 are presented in Table 2. For allosteric activation of CRP by cAMP, the positive cooperativity at both temperatures and pH 7.0 switches to negative cooperativity at the lower temperature and pH 5.2 and to a noncooperative interaction at the higher temperature at pH 5.2. This cooperative behavior is the same as for the activation of T127L by cAMP at both temperatures and pH 5.2. The switch from negative to noncooperativity at the higher temperature is determined by differences in the heat capacity change (ΔC_p) accompanying cAMP binding to the first subunit and then binding to the second subunit, as shown in Table 2. Values for ΔC_p from cAMP binding to the first subunit in CRP and T127L are negative at both pH levels. However, for binding to the second subunit, they change from a negative value at pH 7.0 to a positive value at pH 5.2. Values of ΔC_p can yield information on the conformational changes in CRP and in T127L accompanying cAMP binding to the second subunit via the relationship (*16*):

$$\Delta C_p \,(\mathrm{J\ mol^{-1}\ K^{-1}}) = (188 \pm 8)\Delta \mathrm{SA_{np}} - (109 \pm 13)\Delta \mathrm{SA_p} \quad (5)$$

where ΔSA_{np} is the change in the solvent-accessible surface area of the nonpolar residues and ΔSA_p is the change in the solvent-accessible surface area of the polar residues. The heat capacity changes are negative for binding to the first subunit over the pH range from 5.2 to 7.0, implying a decrease in the solvent-accessible surface area of the nonpolar residues and/or an increase in the solvent-accessible surface area of the polar residues of CRP. However, for cAMP binding to the second subunit, values of ΔC_p change from a negative value at pH 7.0 to a positive value at pH 5.2. This implies that the conformational change resulting from cAMP binding to the second subunit in CRP is different at the lower pH and results from either an increase in the solvent-accessible surface area of the nonpolar residues or/and a decrease in the solvent-accessible surface of the polar residues. For cAMP binding to the second subunit of T127L, it is also positive, implying that the same conformational change may occur at the lower pH. The conformational change upon cAMP binding to the first subunit of CRP is apparently the same at both pH levels. In contrast, values of ΔC_p for cGMP binding to each subunit of T127L (-0.9 ± 0.2 kJ mol^{-1} K^{-1} at pH 5.2 and -0.7 ± 0.1 kJ mol^{-1} K^{-1} at pH 7.0) and for cAMP binding to each subunit of S128A remain the same (0.9 ± 0.2 kJ mol^{-1} K^{-1}) at each pH level. The conformational changes accompanying cGMP binding to T127L and cAMP binding to S128A, apparently, are the same at both pH levels.

To further explore the nature of this change in the allosteric activation of T127L by cAMP at the lower pH, the level of allosteric activation was determined from ITC measurements on the binding of conDNA, a 40 bp duplex which contains a 22 bp promoter sequence that best represents the promoter CRP binding site sequences of the 25 operons, to cAMP-ligated T127L at pH 5.2. The level of activation in terms of the binding affinity of conDNA is about the same, $K_b = (7 \pm 1) \times 10^4$ M^{-1} at pH = 7.0 (*6*) and $(1.1 \pm 0.4) \times 10^5$ M^{-1} at pH = 5.2. The value at pH = 5.2 still indicates activation of T127L by cAMP since it is the same as that of DNA containing the *lac* promoter sequence binding to cAMP-ligated T127L (*6*). However, the higher conDNA binding enthalpy of 131 ± 20 kJ mol^{-1} at pH = 5.2 versus 84 ± 4 kJ mol^{-1} at pH = 7.0 (*6*) is compensated by a higher binding entropy at pH = 5.2. A DNA binding-site conformation different than the binding-site conformation at pH = 7.0 would account for these differences in the binding enthalpy and entropy. Any protonation on the surface of the protein at the DNA binding site, particularly at His159 and His199, would have very little effect on the binding affinity since at the high ionic strength of 0.5 KCl in the buffer these charges are effectively shielded.

DSC Measurements. At pH 7.0, CRP, T127L, and S128A exhibit a single denaturation peak, as shown by the DSC scan of T127L in Figure 5. Although the mutant transitions, like that of CRP (*17*), do not reappear upon a rescan of the sample, the thermal transition thermodynamic quantities of the mutants are independent of scan rate from 8 to 80 K h^{-1} and concentration as shown in Table 3 and, thus, can be

Table 3: Thermodynamic Quantities of the Thermal Unfolding of CRP/Mutants as a Function of pH from DSC Measurements[a]

CRP mutant	concn (mM)	pH	T_m (°C)	$\Delta_{trs}H_v$ (kJ mol^{-1})	$\Delta_{trs}H_c$ (kJ mol^{-1})	$\Delta_{trs}H_c/\Delta_{trs}H_v$
CRP	0.05−0.20	7.0	65.6 ± 0.3	1054 ± 104	328 ± 7	0.31 ± 0.03
		6.0	64.9 ± 0.1	885 ± 22	372 ± 8	0.42 ± 0.01
		5.2	57.7 ± 0.1	668 ± 56	332 ± 43	0.50 ± 0.08
		4.6	55.2 ± 0.4	554 ± 16	289 ± 36	0.52 ± 0.03
S128A	0.068−0.26	7.0	65.4 ± 0.2	1034 ± 51	378 ± 35	0.37 ± 0.04
	c		64.9 ± 0.2	900 ± 20	400 ± 30	(0.44 ± 0.03)[b]
	d		65.2 ± 0.5	986 ± 50	420 ± 21	0.43 ± 0.03)
	e		64.3 ± 0.5	780 ± 40	440 ± 23	(0.56 ± 0.04)
		6.0	65.0 ± 0.1	878 ± 5	375 ± 5	0.43 ± 0.01
		5.2	57.5 ± 0.3	643 ± 17	279 ± 38	0.43 ± 0.06
		4.6	54.1 ± 0.4	665 ± 39	222 ± 2	0.33 ± 0.02
T127L	0.04−0.56	7.0	66.6 ± 0.2	667 ± 30	240 ± 61	0.36 ± 0.09
	c		65.8 ± 0.7	618 ± 30	270 ± 27	(0.44 ± 0.04)
	d		66.4 ± 0.5	694 ± 35	310 ± 15	(0.45 ± 0.03)
	e		67.0 ± 0.5	590 ± 20	220 ± 20	(0.43 ± 0.04)
		6.0	66.5 ± 0.3	500 ± 10	339 ± 3	0.68 ± 0.02
		5.2	54.9 ± 0.1	907 ± 9		
			60.0 ± 0.1	575 ± 21	354 ± 4	
		4.6	50.2 ± 1.6	498 ± 61		
			58.3 ± 0.8	538 ± 27	249 ± 9	

[a] The uncertainties are standard uncertainties as described in the text. [b] The results in parentheses are values determined at the specified scan rates, while the other results are averages from two to three determinations at several scan rates. [c] At a scan rate = 8.0 K h^{-1}. [d] At a scan rate = 13.0 K h^{-1}. [e] At a scan rate = 80.0 K h^{-1}.

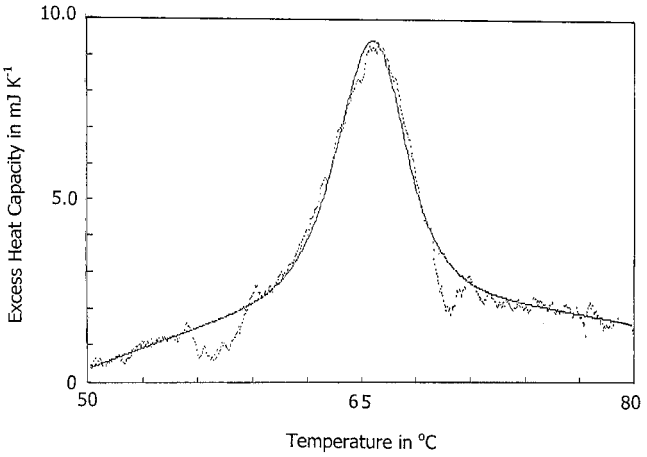

FIGURE 5: DSC scan of 0.156 mM T127L in potassium phosphate buffer (pH 7.0) solution. The solution sample mass is 0.5 g, and the scan rate is 20 K h^{-1}.

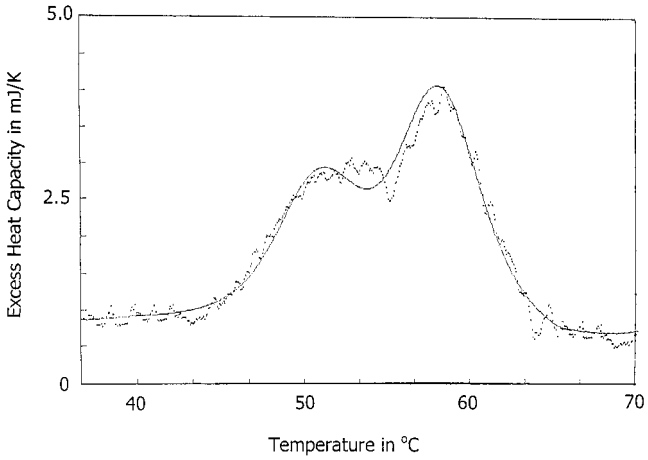

FIGURE 6: DSC scan of 0.133 mM T127L in acetate buffer (pH 5.2) solution. The solution sample mass is 0.5 g, and the scan rate is 20 K h^{-1}.

determined from application of a two-state transition model, A↔B, to the DSC data (also shown in Figure 5). Ghosaini et al. (*17*) determined values of T_m = 66.4 ± 0.1 °C and $\Delta_{trs}H_v$ = 963 ± 32 kJ mol^{-1}, which were independent of scan rate and concentration of CRP, and are close to the corresponding values of 65.6 ± 0.3 °C and 1054 ± 104 kJ mol^{-1} in Table 3. However, the value for $\Delta_{trs}H_c$ of 544 ± 24 kJ mol^{-1} from Ghosaini et al. (*17*) is higher than the corresponding value of 328 ± 8 kJ mol^{-1} in Table 3. This lower value yields a ratio of $\Delta_{trs}H_c/\Delta_{trs}H_v$ = 0.31 ± 0.03 in Table 3 compared to the value from Ghosaini et al. (*16*) of 0.56, from which it was concluded that CRP exists as a dimer (tetramer if considering the monomer subunits) at the transition temperature (*17*). Values of T_m, $\Delta_{trs}H_v$, and $\Delta_{trs}H_c$ for the S128A mutant are the same as those for CRP at pH 7.0. However, for T127L, the T_m is 66.6 ± 0.2 °C, higher than that of CRP and S128A, $\Delta_{trs}H_v$ is almost half of the $\Delta_{trs}H_v$ values for CRP and S128A, and $\Delta_{trs}H_c$ is slightly lower, 240 ± 61 kJ mol^{-1}, than the $\Delta_{trs}H_c$ values for CRP and S128A. The higher thermal stability of the T127L mutant is also evident at pH 6.0, where the T_m is 1.5 °C higher than the T_m values for CRP and S128A. The lower $\Delta_{trs}H_c/\Delta_{trs}H_v$ ratios of 0.4 for S128A and T127L at pH 7.0 also indicate, as with CRP, the mutants exist as dimers at T_m.

The DSC scans of T127L also exhibit a unique dependence on pH. While only a single transition peak is observed for the thermal denaturation of CRP and S128A in the pH range from 7.0 to 4.6, at pH 5.2 and below, the denaturation of T127L consists of two transition peaks with transition temperatures 5−8 °C apart, as shown in Figure 6. Both CRP and S128A exhibit monotonic decreases in T_m, $\Delta_{trs}H_v$, and $\Delta_{trs}H_c$ as the pH is lowered from 7.0 to 4.6, which results from destabilization of its native state because of an increase in charges on the surface of the protein. This is also observed in the denaturation of the simpler globular proteins, lysozyme and ribonuclease A (*18*). Values of T_m for the two transitions of T127L also decrease with decrease in the pH. The mean temperature of the two transitions is the same as the transition temperatures of S128A and CRP at pH 5.2 and 6.0. The two transition peaks of T127L at pH 4.6 and 5.2 are indicative of two thermodynamic domains in the protein unfolding independently. This is similar to the observation of three

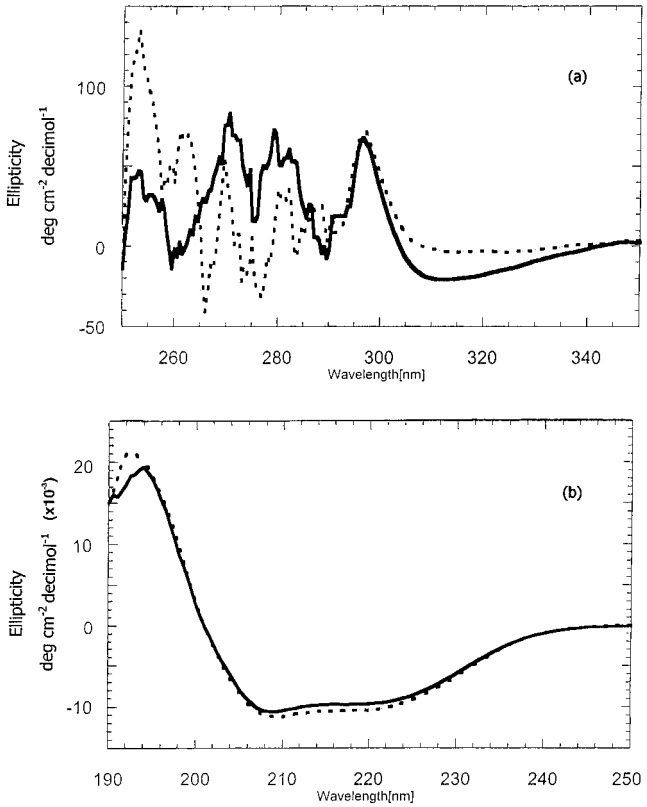

FIGURE 7: (a) Near-UV CD spectrum of 0.125 mM CRP at pH 7.0 (—) and at pH 5.2 (- - -). (b) Far-UV CD spectrum of 0.125 mM CRP at pH 7.0 (—) and at pH 5.2 (- - -).

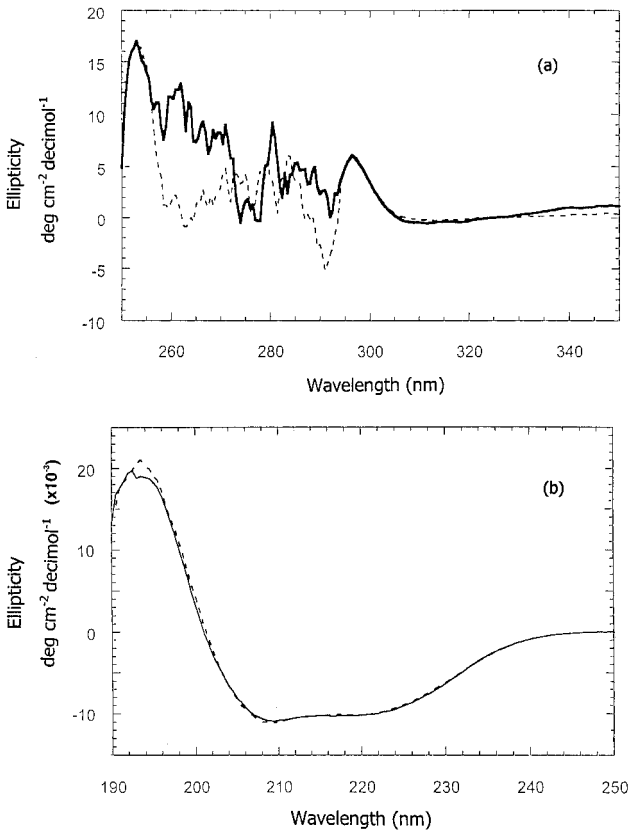

FIGURE 8: (a) Near-UV CD spectrum of 0.125 mM T127L at pH 7.0 (—) and at pH 5.2 (- - -). (b) Far-UV CD spectrum of 0.125 mM T127L at pH 7.0 (—) and at pH 5.2 (- - -).

transition peaks and two transition peaks in the denaturation of CRP in the presence of, respectively, cAMP and cGMP (*17*). DSC scans of the mutants in the presence of cGMP and cAMP at neutral pH, however, exhibited only one transition peak with a T_m which increased with increase in the cNMP concentration, as would be expected for ligand binding to only the native state. The lower value of $\Delta_{trs}H_v$ for T127L at pH 7.0, despite the higher transition temperature, is indicative of a transition broader than that of CRP or S128A, which may be due to the merging of two transitions at this pH. Changes in the thermal denaturation of T127L over this pH range reflect changes in the structure of T127L, which may also be responsible for the change in the allosteric activation of T127L by cAMP over this range. In contrast, the thermal denaturations of CRP and S128A are consistent with little change in the structure of these proteins over this pH range.

CD Results. Typical CD spectra of CRP and T127L at pH 7.0 and 5.2 above 250 nm are shown, respectively, in Figures 7 and 8. Below 250 nm at pH 5.2 and 7.0, the CD spectra are the same, which indicates very little change in the α-helical structure of both proteins over this pH range. However, as shown in Figures 7 and 8, the CD spectra above 250 nm exhibit different changes over this pH range, resulting from changes in the tertiary structure. Changes in the tertiary structure would include interactions between the α-helices in the carboxyl-terminal domain and between the α-helices and β-pleated sheets of the amino-terminal domain of the protein, as well as changes in the interaction between the carboxyl- and amino-terminal domains of the protein. The absorption peak at 295 nm is the same for both proteins at pH 5.2 and 7.0, which can be interpreted that the tertiary

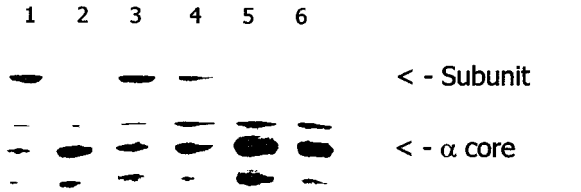

FIGURE 9: Comparison of proteolysis fragmentation patterns by subtilisin at pH 5.2 where lane 1 is the enzyme with CRP, cAMP-ligated CRP in lane 2, cGMP-ligated CRP in lane 3, T127L in lane 4, cAMP-ligated T127L in lane 5, and cGMP-ligated T127L in lane 6.

structure around the two tryptophan residues in the amino-terminal domain remains the same as the pH is reduced from 7.0 to 5.2. Thus, it appears that changes in the tertiary structure occur in the carboxyl-terminal domain or in the interaction between the carboxyl- and amino-terminal domains for both proteins over this pH range. These changes in the tertiary structure of T127L are different than those of CRP and may be responsible for the change in the allosteric activation of T127L by cAMP over the pH range from 7.0 to 5.2.

Proteolysis Results. The results of the proteolysis of CRP and T127L by subtilisin at pH 5.2 are presented in Figure 9. All the solution samples exhibit a band at 14 500 g mol^{-1}, termed the α-core band. Only CRP, cGMP-ligated CRP, and T127L exhibit the subunit band at 22 500 g mol^{-1}, indicating that the subunits maintain their structural entities as subunits. The lack of this band for cAMP-ligated CRP and cNMP-ligated T127L indicates that ligand-induced structural changes in these complexes increase the subunit association interac-

tion to the extent that the subunits no longer exist as distinct structural entities. Commensurate with this loss of subunit structural integrity is the observation that all three complexes are allosterically activated. These three complexes also exhibit, through to a different degree, a three-band fragmentation pattern. This is also in contrast to CRP, cGMP-ligated CRP, and T127L, which exhibit the same four-band fragmentation pattern, although the intensities of the three lower molecular mass bands of CRP are much less than those of cGMP-ligated CRP and T127L.

DISCUSSION

In the X-ray crystal structure of cAMP-ligated CRP, one subunit is in an "open" form, where the carboxyl-terminal domain is swung out away from the amino-terminal domain and subunit interface, while the other subunit is in a "closed" form, where the carboxyl-terminal domain is swung in toward the amino-terminal domain and subunit interface (*19*). The transition from one form to the other form occurs via a "hinge" region (residues 130−139) connecting the carboxyl-terminal domain with the α-helical subunit interface. Mutations near this region also affect the allosteric activation of CRP by cNMP (*7*). Both subunits are in the closed form when the cAMP-ligated CRP complex is bound to a DNA duplex containing the promoter CRP binding site sequence (*1*). Minimum energy calculations on CRP, either in the exclusively closed or in the open form, show that the minimum energy conformation of cAMP-ligated CRP is the closed form in solution, indicating that this is the dominant conformation of cAMP-ligated CRP (*20*). Small-angle neutron scattering (SANS) measurements on CRP and cAMP-ligated CRP in solution showed that unligated CRP exists exclusively in the open form and that the radius of gyration of CRP is reduced upon allosteric activation by cAMP (*21*). The X-ray structures, minimum energy calculations, and SANS results imply that the allosteric activation of CRP by cAMP involves a conformational change where CRP converts from an exclusively open form to a closed form. Binding of cAMP to CRP increases the intersubunit interaction as indicated by the decrease in the radius of gyration of CRP upon binding of cAMP in the SANS data (*21*) and by reduction of the subunit exchange rates in the presence of cAMP at low CRP concentrations (*5*). The T127→L mutation modifies the subunit interface to a more perfect leucine-zipper motif and, thus, would increase the intersubunit association. The higher thermal stability of T127L than that of CRP and S128A, even at T_m by 1.5 °C, may be attributed to a stronger subunit association. Similarly, the T127→C mutation induces a disulfide bond across the subunit−subunit interface, which would also enhance the intersubunit association (*4*). Both mutants undergo allosteric activation by cAMP and cGMP, implying that the need for specific groups on the purine ring of cAMP to increase the intersubunit association is fulfilled in part by the leucine-zipper motif in T127L and the disulfide bond in T127C. Additional mutations of T127→ G, I, and S, which do not contribute to the intersubunit association, are not allosterically activated by cAMP to bind to the *lac* promoter site (*4*). An increase in the intersubunit association, whether through cAMP binding or mutations along the subunit interface (T127→L, C), converts the CRP from the open to the active tighter binding closed form and the T127L to a form more closely related to the closed form, which can account for the DSC and proteolysis results. The DSC scan of CRP, which is in the open form, consists of a single transition, and cAMP-ligated CRP, which is in the closed form, consists of three transitions (*17*). Similarly, the DSC scan of T127L at low pH consists of two transitions, which would also account for the broadness of the transition at pH 7.0. The tighter binding subunits of the T127L mutant would induce unfolding of both amino-terminal domains as a single entity to account for one transition in T127L, while unfolding of the carboxyl-terminal domains would account for the other transition. Since the number of protonated histidine residues from 1 to 98 is twice those from 98 to 205, greater thermal destabilization at lower pH would occur with the amino-terminal domains and, thus, two unfolding transitions become resolvable into unfolding of the protonated amino-terminal domain at the lower temperature and unfolding of the protonated carboxyl-terminal domain at the higher temperature. In contrast, the thermal denaturation of the S128A mutant, like that of CRP, consists of a single transition throughout the pH range from 5.2 to 7.0. Proteolysis of the allosterically activated cAMP-ligated CRP and cNMP-ligated T127L complexes, which are exclusively in the closed form, at pH 5.2 does not yield the subunit product bands. Changes accompanying the transition from an open form to a closed form would be particularly important in the tertiary structure of the carboxyl-terminal domains compared to the tertiary structure of the amino-terminal domains. This implies that at neutral pH, the tertiary structure of the carboxyl-terminal domains of T127L is close to that of the allosterically activated closed form.

The change in the allosteric activation of T127L by cAMP from an exothermic independent two-site binding mechanism at pH 7.0 to an endothermic, interacting two-site binding mechanism at pH 5.2 implies that the partial conformation of T127L in the closed form, induced by the T127→L mutation, is compensated by another mechanism at pH 5.2 and the activation mechanism of CRP is partially restored. This partial restoration is also evident in the similarities in the heat capacity changes and the cooperativity of the allosteric activation of CRP and T127L by cAMP at the lower pH. In addition, the heat capacity change for binding to the second subunit of CRP switches from a negative value at pH 7.0 to a positive value at pH 5.2, where a positive value is also observed for cAMP binding to the second subunit of T127L. This alteration in the heat capacity change of CRP implies that the conformational change accompanying binding to the second subunit of CRP also changes with pH. In contrast, heat capacity changes accompanying cAMP binding to the first and second subunits of S128A remain the same at pH 5.2 and 7.0 as well as the exothermicity of this binding reaction. The cooperativity of the allosteric activation of CRP by cAMP is also reduced from 5 at pH 7.0 to below 1.0 at pH 5.2, a level of cooperativity that is also observed for the allosteric activation of T127L by cAMP at this pH. As the pH is decreased from 7.0 to 5.2, the most likely amino acids to become protonated are the histidine residues that are homogeneously dispersed on the surface of the subunits opposite the monomer−monomer interface. However, due to ion shielding, this protonation is expected to have little effect on the subunit−subunit interaction, and, thus, the partial restoration of the endothermic allosteric

activation mechanism in T127L does not involve a weakening of the subunit interaction with pH. The effect of ion shielding is apparent in the levels of allosteric activation by cAMP at pH 7.0 and 5.2, as determined from comparison of the conDNA binding affinities. The binding affinity at pH = 5.2 is the same as at pH = 7.0 although the binding enthalpy and binding entropy are higher at pH = 5.2. If electrostatic effects are more involved in the binding reaction at the lower pH, then there would be a change in the binding affinity at the lower pH. The increase in the endothermicity of the binding reaction at pH 5.2 arises out of changes in the structure of the carboxyl-terminal domains to a conformation less favorable toward DNA binding, i.e., poorer alignment of the α-helices in the carboxyl-terminal domain with the major groves of the DNA helix. Conformational changes in the carboxyl-terminal domain over this pH range are evident in the CD results and the proteolysis products. The CD results can be interpreted that the observed changes in the tertiary structures of T127L and CRP with pH do not involve the tryptophan residues at positions 13 and 35 in the amino-terminal domain, implying that the tertiary structure of this terminal domain is unaffected by change in pH. The relative stability of the amino-terminal domain to changes in pH is observed in the proteolysis results where the α core, mainly encompassing the amino-terminal domain, is always observed as a major product for cAMP-ligated complexes of CRP and cNMP-ligated T127L at pH 5.2 and 7.0 (*2*). In earlier studies (*22*), the α core fragment was isolated and shown to bind cAMP, implying that proteolysis by subtilisin does not alter the conformation of the cAMP binding site in the amino-terminal domain. The implication is that the change in pH affects the tertiary structure of the carboxyl-terminal domains in T127L to the extent that they approach the tertiary structure of the carboxyl-terminal domains of CRP at the lower pH. This structural change in T127L restores the tertiary structure of the carboxyl-terminal domain of CRP in the open form and, thus, the endothermic allosteric activation mechanism of CRP, while maintaining the tighter intersubunit association in T127L.

REFERENCES

1. Schultz, S. C., Shields, G. C., and Steitz, T. A. (1991) *Science 253*, 1001−1007.
2. Moore, J. L. (1993) *The Mechanism of Activation of the Escherichia coli Cyclic AMP Receptor Protein by Cyclic AMP*, Ph.D. Thesis, The George Washington University, Washington, DC.
3. Lee, E. J., Glasgow, J., Leu, S. F., Belduz, A. O., and Harman, J. G. (1994) *Nucleic Acids Res. 22*, 2894−2901.
4. Leu, S. F., Baker, C. H., Lee, E. J., and Harman, J. G. (1999) *Biochemistry 38*, 6222−6230.
5. Brown, A. M., and Crothers, D. M. (1989) *Proc. Natl. Acad. Sci. U.S.A. 86*, 7387−7391.
6. Shi, Y., Wang, S., Krueger, S., and Schwarz, F. P. (1999) *J. Biol. Chem. 274*, 6946−6956.
7. Cheng, X., and Lee, J. C. (1999) *Biochemistry 38*, 51−60.
8. Gorshkova, I., Moore, J. L., McKenney, K. H., and Schwarz, F. P. (1995) *J. Biol. Chem. 270*, 21679−21683.
9. Moore, J. L., Gorshkova, I., Brown, J. W., McKenney, K. H., and Schwarz, F. P. (1996) *J. Biol. Chem. 271*, 21273−21278.
10. Zhang, X., Zhou, Y., Ebright, Y., and Ebright, R. H. (1992) *J. Biol. Chem. 267*, 8136−8139.
11. Wiseman, T., Williston, S., Brandts, J. F., and Lin, L. N. (1989) *Anal. Biochem. 179*, 131−137.
12. Yang, C. P. (1990) *Omega Data in Origin*, p 66, Microcal, Inc., Northhampton, MA.
13. Schwarz, F. P., and Kirchhoff, W. H. (1988) *Thermochim. Acta 128*, 267−295.
14. Chakrabarti, M. C., and Schwarz, F. P. (1999) *Nucleic Acids Res. 27*, 4801−4806.
15. Kirchhoff, W. H. (1993) *Exam*: *A Two-State Thermodynamic Analysis Program*, NIST Technol. Note 1401, pp 1−103.
16. Murphy, K. P., Dong Xie, Garcia, K. C., Amzel, L. M., and Freire, E. (1993) *Proteins*: *Struct., Funct., Gent. 15*, 113−120.
17. Ghosaini, L. R., Brown, A. M., and Sturtevant, J. M. (1988) *Biochemistry 27*, 5258−5261.
18. Privalov, P. L. (1979) *Adv. Protein Chem. 33*, 167−242.
19. McKay, D. B., Weber, I. T., and Steitz, T. A. (1982) *J. Biol. Chem. 257*, 9518−9524.
20. Garcia, A. E., and Harman, J. G. (1996) *Protein Sci. 5*, 62−71.
21. Krueger, S., Gorshkova, I., Brown, J., Hoskins, J., McKenney, K. H., and Schwarz, F. P. (1998) *J. Biol. Chem. 273*, 20001−20006.
22. Angulo, J., and Krakow, J. S. (1986) *J. Biol. Chem. 261*, 11315−11319.

BI000225M